Journal of Sol-Gel Science and Technology (2023) 108:392–400
https://doi.org/10.1007/s10971-023-06184-w

ORIGINAL PAPER

Formation of a molecularly and mesoscopically ordered structure from cage siloxanes with a long alkyl chain and dimethylsilanol groups

Yuta Hattori[1] · Taiki Hayashi[1] · Takuya Hikino[2] · Ryuta Miwa[1] · Yosuke Oka[1] · Koki Fujino[1] · Naoto Sato[1] · Takamichi Matsuno[1,3] · Hiroaki Wada[1,3] · Kazuyuki Kuroda[1,3] · Atsushi Shimojima[1,3]

Received: 13 May 2023 / Accepted: 27 June 2023 / Published online: 27 July 2023

Abstract

Structural control of siloxane-based materials at multiple length scales is important for various applications. In this study, we report the controlled assembly of cage oligosiloxane building blocks by both intermolecular hydrogen bonding and hydrophobic interactions. A cage siloxane molecule modified with seven dimethylsilanol groups and an octadecyldimethylsilyl group was synthesized by stepwise silylation of double-four-ring (D4R) cage octasilicate anions. This molecule self-assembled to form a molecularly and mesoscopically ordered structure by solvent evaporation. Furthermore, the silanol groups in the assembled solids were cross-linked by silylation with dichlorodimethylsilane. This approach will allow for the creation of various hierarchically ordered siloxane-based materials by molecular design.

Graphical Abstract

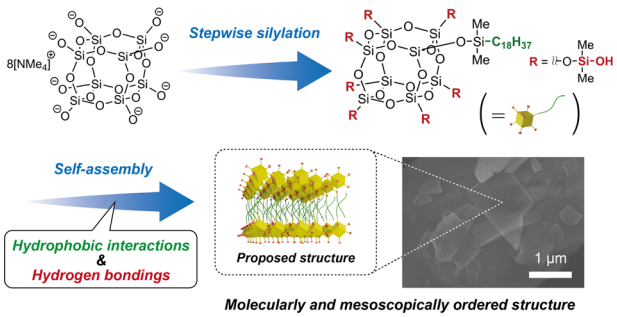

Keywords Cage siloxane · Silylation · Silanol groups · Hydrogen bonds · Self-assembly

Highlights

- A cage siloxane molecule containing seven dimethylsilanol groups and an octadecyldimethylsilyl group was synthesized.
- The cage siloxane molecules formed an ordered solid with both molecular and mesoscale periodicities by self-assembly.
- The silanol groups in the ordered solid were cross-linked by dichlorodimethylsilane to form siloxane networks.

These authors contributed equally: Yuta Hattori, Taiki Hayashi

✉ Atsushi Shimojima
shimojima@waseda.jp

[1] Department of Applied Chemistry, Faculty of Science and Engineering, Waseda University, 3-4-1 Okubo, Shinjuku-ku, Tokyo 169-8555, Japan

[2] Department of Advanced Science and Engineering, Faculty of Science and Engineering, Waseda University, 3-4-1 Okubo, Shinjuku-ku, Tokyo 169-8555, Japan

[3] Kagami Memorial Research Institute for Materials Science and Technology, Waseda University, 2-8-26 Nishiwaseda, Shinjuku-ku, Tokyo 169-0051, Japan

1 Introduction

Ordered siloxane-based materials composed of regularly arranged SiO_4 tetrahedral units are useful for various applications, including catalysis and adsorption [1]. Crystalline silicates such as zeolites [2] and layered silicates [3] are generally synthesized by hydrothermal treatments, but the complex crystallization mechanism makes it difficult to precisely control the structure and compositions. Controlled assembly of pre-designed molecular building blocks is a promising method to expand the structural and compositional diversity of molecularly ordered siloxane-based materials. Among various types of oligosiloxanes with well-defined structures [4–10], cage siloxanes have attracted particular attention as building blocks because of their rigid frameworks and various functional groups at the corners [7, 8]. Extensive studies have been made on cross-linking of cage siloxanes via Si–O–Si bonds and organic linkers [11, 12]; however, most of the materials have random network structures, and controlled assembly of cage siloxanes has been an important issue.

The use of intermolecular interactions is crucial to realize the assembly of oligosiloxanes into molecularly ordered structures. Hydrogen bonds (H-bonds) of silanol groups are quite effective for the regular assembly of cage siloxanes. Several different arrangements of octa-silanol modified cage siloxanes, from one-dimensional (1D) to three-dimensional (3D) assemblies, have been reported [13–19]. The silanol groups are also useful for intermolecular linking by the formation of Si–O–Si bonds either by dehydration condensation or by silylation. We have recently synthesized H-bonded molecular crystals of cage siloxanes modified with SiR_2OH groups (R = Me and ^{i}Pr) [16–19]. Furthermore, cross-linking of the H-bonded $SiMe_2OH$ groups of the cage siloxanes was achieved by silylation with trichlorosilane, resulting in the formation of a crystalline microporous material [17]. Nevertheless, the crystalline structures assembled from octa-silanol modified cage siloxanes have been still limited, and the formation of mesoscale structures remains a challenge.

Introducing organic substituents to the corner Si atoms of cage siloxanes allows mesoscale assembly. Polyhedral oligomeric silsesquioxanes (POSS, $R_8Si_8O_{12}$, R = H or organic groups) modified with various organic functional groups and/or polymers were designed to drive hierarchical assembly into complex architectures [20–22]. However, the regularity of the cage siloxanes was not well-controlled in many cases. In addition, most of these POSS-based assemblies cannot be cross-linked by siloxane networks, except for those having SiH groups [20]. On the other hand, we reported the formation of lamellar and two-dimensional (2D) hexagonal mesostructures by the sol–gel reactions of cage siloxanes modified with a long-chain alkyl group and seven ethoxy groups [23, 24]. The key step for the self-assembly was hydrolysis of the SiOEt groups into SiOH groups, forming amphiphilic molecules containing silanol groups and a long alkyl group. However, the cage siloxanes were not regularly arranged at the molecular level probably because condensation of the silanol groups partially proceeded prior to self-assembly. Synthesis and isolation of similar amphiphilic siloxane cages modified with relatively stable organosilanol groups and a long alkyl chain are essential.

In this paper, we report the synthesis of a novel cage siloxane compound modified with seven organosilanol groups and a long-chain alkyl group that can form a hierarchical siloxane-based material. Cubic octameric silicate was modified with $SiMe_2H$ groups and a $SiMe_2C_{18}H_{37}$ group by stepwise silylation (**D4R-7SiH** and **D4R-7SiH-C18** in Scheme 1), followed by the conversion of the $SiMe_2H$ groups to $SiMe_2OH$ groups using a Pd/C catalyst (**D4R-7SiOH-C18**). Upon solvent evaporation, the molecule was assembled to form a crystalline solid with a regular arrangement of the cages induced by the intermolecular H-bonding of the silanol groups and a mesoscale periodicity induced by the long alkyl chains. Furthermore, cross-

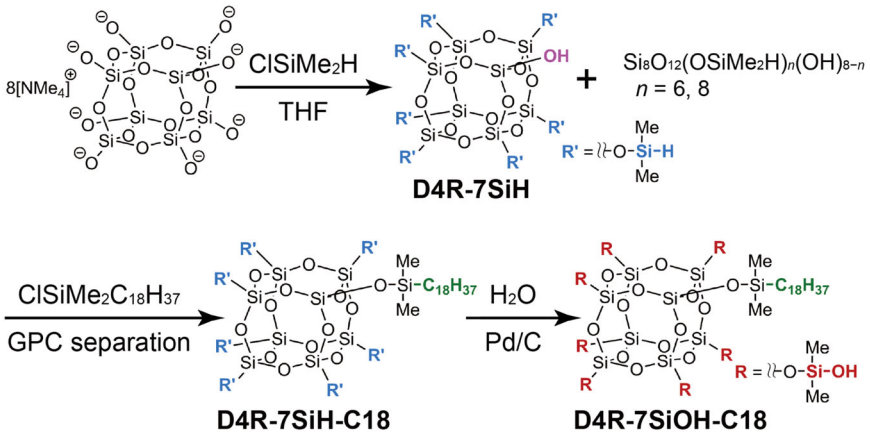

Scheme 1 Synthetic route to cage siloxane modified with a long alkyl chain and organosilanol groups (**D4R-7SiOH-C18**) starting from cubic octameric silicate

linking of the silanol groups by siloxane bonds was performed by silylation with dichlorodimethylsilane.

2 Experimental

2.1 Materials

The following reagents were used as received: acetonitrile (FUJIFILM Wako Pure Chemical Co., >99.5%), chlorodimethylsilane (DMSCl, Sigma-Aldrich, >97.5%), chloroform (FUJIFILM Wako Pure Chemical Co., >99.0%), chloro(octadecyl)dimethylsilane (C_{18}DMSCl, Tokyo Chemical Industry Co. Ltd., >97.0%), dichlorodimethylsilane (Tokyo Chemical Industry Co. Ltd., >98.0%), diethyl ether (FUJIFILM Wako Pure Chemical Co., >99.5%), ethanol (Junsei Chemical Co. Ltd., 99.5%), hexane (Kanto Chemical Co. Inc., >99.0%), methanol (FUJIFILM Wako Pure Chemical Co., >99.8%), magnesium sulfate (anhydrous, FUJIFILM Wako Pure Chemical Co., >98.0%), pyridine (dehydrated, FUJIFILM Wako Pure Chemical Co., >99.5%), tetraethylorthosilicate (TEOS, FUJIFILM Wako Pure Chemical Co., >95.0%), tetrahydrofuran (THF, stabilizer free, Wako Pure Chemical Industries Ltd., >99.5%), tetramethylammonium hydroxide pentahydrate (TMA hydroxide·5H_2O, Tokyo Chemical Industry Co. Ltd., >97.0%), and Pd/C (type STD (Pd 5%) (wetted with water), Manufacturer: N.E. CHEMCAT, FUJIFILM Wako Pure Chemical Co.).

2.2 Synthesis of cubic octameric silicate

Tetramethylammonium silicate with a D4R structure ($TMA_8Si_8O_{20}$·xH_2O) was synthesized according to our previous report [25]. TEOS (61.8 mL) was added to the mixture of TMA hydroxide·5H_2O (50 g), ethanol (160.6 mL), and H_2O (24.8 mL). The molar ratio was TEOS: TMA hydroxide: ethanol: H_2O = 1: 1: 10: 10. After stirring for 3 d, the solution was concentrated to about half of the original volume by heating on a hot plate. The hydrated crystals precipitated upon cooling were filtrated and vacuum dried at room temperature to obtain a white solid (54.1 g). ^{29}Si nuclear magnetic resonance (NMR) (99.37 MHz, ethanol-d_6): δ (ppm) −99.00 ($Si(OSi)_3O^-$). Thermogravimetry (TG)-differential thermal analysis (DTA) revealed that the weight loss was 72% when the final white solid was heated up to 500 °C. Assuming that the residue was SiO_2, the hydration number (x) was calculated to be 32.

2.3 Synthesis of D4R-7SiH

It is reported that incompletely trimethylsilylated and dimethylvinylsilylated cage siloxanes can be obtained by silylation of $Si_8O_{20}^{8-}$ using a THF solvent [26–28]. On the basis of these reports, incomplete dimethylsilylation of cage siloxane was conducted. $TMA_8Si_8O_{20}$·32H_2O (10.6 g) dissolved in methanol (40 mL) was added dropwise to the mixture of THF (100 mL), hexane (100 mL), and DMSCl (12 mL). After stirring for 10 min, H_2O (20 mL) and hexane (200 mL) were added to the reaction mixture. After further stirring for 10 min, the hexane layer was extracted, and the volatile compounds were removed under reduced pressure to obtain a white solid. The solid was washed with acetonitrile (20 mL) by stirring for 10 min to remove cage siloxane containing six or less silylated vertices. Then, a white solid was recovered by filtration (3.1 g, yield: 51% based on the fact that 7.5 corners were silylated on average, as calculated by the ^{29}Si NMR analysis). Although impurities such as $Si_8O_{12}(OSiMe_2H)_6(OH)_2$ and $Si_8O_{12}(OSiMe_2H)_8$ were still contained, the product was used for the subsequent reaction without separation of **D4R-7SiH**.

2.4 Synthesis of D4R-7SiH-C18

D4R-7SiH containing impurities (1.5 g) was dissolved in hexane (40 mL). The solution was added dropwise to the mixture of C_{18}DMSCl (0.54 g), pyridine (190 µL), and hexane (5 mL) in a Schlenk flask under nitrogen atmosphere. After stirring at room temperature for 1 d, DMSCl (3 mL) and pyridine (3 mL) were added. After further stirring at room temperature for 3 h, H_2O (5.0 mL) was added to the reaction mixture and the hexane layer was extracted. Volatile compounds were removed under reduced pressure to obtain a white solid. The solid was dissolved in chloroform and **D4R-7SiH-C18** (a white solid, 0.16 g, yield: 8% based on **D4R-7SiH**) was isolated by gel permeation chromatography (GPC). ^{1}H NMR (500.16 MHz, chloroform-d): δ (ppm) 0.13 (s, 6H; OSi(CH_3)$_2$$C_{18}H_{37}$), 0.22–0.29 (br, 42H; OSi(CH_3)$_2$H), 0.56–0.62 (m, 2H; SiCH_2(CH_2)$_{16}$$CH_3$), 0.88 (t, J = 6.87 Hz, 3H; Si(CH_2)$_{17}$$CH_3$), 1.20–1.40 (br, 32H; SiCH_2(CH_2)$_{16}$$CH_3$), 4.70–4.76 (m, 7H, Si$Me_2H$); ^{13}C NMR (125.77 MHz, THF-d_8): δ (ppm) 0.39, 0.45, 0.48, 14.51, 18.07, 23.11, 23.35, 29.79, 29.82, 30.09, 30.13, 32.36, 33.86; ^{29}Si NMR (99.37 MHz, chloroform-d): δ (ppm) 13.41, −1.47, −1.59, −108.57, −108.61, −108.66, −109.06.

2.5 Synthesis and self-assembly of D4R-7SiOH-C18

D4R-7SiH-C18 (0.30 g) was dissolved in THF (10 mL) under nitrogen atmosphere. Pd/C (20 mg) and H_2O (50 µL) were added to the solution. After stirring for 1 d at 40 °C, anhydrous magnesium sulfate was added and filtered through Celite®. The volatile compound was removed using a rotary evaporator to give a white solid (0.32 g, yield: 98%). ^{1}H NMR (500.16 MHz, THF-d_8): δ (ppm) 0.10 (s,

42H; $OSi(CH_3)_2OH$), 0.14 (s, 6H; $OSi(CH_3)_2C_{18}H_{37}$), 0.60–0.65 (m, 2H; $SiCH_2(CH_2)_{16}CH_3$), 0.88 (t, $J = 6.87$ Hz, 3H; $Si(CH_2)_{17}CH_3$), 1.22–1.38 (br, 32H; $SiCH_2(CH_2)_{16}CH_3$), 5.5–5.6 (br, 3H, $SiMe_2OH$), 5.6–5.7 (br, 4H, $SiMe_2OH$); ^{13}C NMR (125.77 MHz, THF-d_8): δ (ppm) 0.21, 0.27, 0.35, 14.61, 18.64, 23.69, 24.05, 30.44, 30.49, 30.74, 30.79, 30.85, 33.00, 34.61; ^{29}Si NMR (99.37 MHz, THF-d_8): δ (ppm) 12.77, −11.28, −11.37, −11.66, −108.67, −109.42, −109.45, −109.59.

D4R-7SiOH-C18 (0.13 g) was dissolved in diethyl ether (2 mL) and the solution was added over 5 mL of H_2O in a 15 mL sample bottle. During evaporation of diethyl ether at room temperature for 3 d, crystalline solids were formed on the top of the H_2O layer. The solids were collected by filtration.

2.6 Cross-linking of D4R-7SiOH-C18

A mixture of hexane (10 mL) and dichlorodimethylsilane (18 µL) was added to the crystal of **D4R-7SiOH-C18** (50 mg) under nitrogen atmosphere. After standing at room temperature for 1 d, solids were collected by filtration (24 mg).

2.7 Characterization

Liquid-state ^{1}H, ^{13}C, and ^{29}Si NMR spectra were recorded on a JEOL JNM ECZ 500 spectrometer at resonance frequencies of 500.0 MHz, 125.7 MHz, and 99.4 MHz, respectively, at ambient temperature using 5 mm glass tubes. Tetramethylsilane was used as an internal reference (set as 0 ppm). Chloroform-d, ethanol-d_6, and THF-d_8 were used to obtain lock signals. ^{29}Si NMR spectra were measured with a 45° pulse and a recycle delay of 30 s. Solid-state ^{13}C cross-polarization (CP)/magic-angle spinning (MAS) NMR and ^{29}Si MAS NMR spectra were recorded on a JEOL JNM ECA 400 spectrometer at resonance frequencies of 100.53 MHz and 79.43 MHz, respectively, at ambient temperature. The sample was put in a 5 mm zirconia rotor. Fourier transform infrared (FT-IR) spectra were recorded on a JASCO FT/IR-6100 spectrometer using the KBr method. X-ray diffraction (XRD) patterns were recorded on a Rigaku Ultima-III diffractometer with a parallel beam geometry equipped with a scintillation detector and parabolic multilayer mirror using Cu Kα radiation ($\lambda = 1.5418$ Å). GPC was carried out using a Japan Analytical Industry LC-7080 system equipped with a refractive index detector RI-700LA. JAIGEL-HR series columns (1HR, 2HR, and 2HR plus) were used with chloroform as the eluent at a flow rate of 7.0 mL min^{-1}. Matrix-assisted laser desorption ionization time-of-flight (MALDI-TOF) mass analysis was conducted using a Bruker autoflex maX instrument with dithranol as the matrix and sodium trifluoroacetate as the ionization aids. Scanning electron microscopy (SEM) images were obtained on a Hitachi S5500 electron microscope with an accelerating voltage of 1–5 kV. Transmission electron microscopy (TEM) images and selected area electron diffraction (SAED) patterns were obtained on a JEOL JEM-2010 microscope with an accelerating voltage of 200 kV. Samples for TEM and SEM analyses were dispersed on a carbon-coated Cu grid (Okenshoji Co., Ltd.). Cross-sectional sample was prepared using a focused ion beam (FIB) milling and imaging system (JIB-4700) equipped with an FIB and a scanning ion microscope. **D4R-7SiOH-C18** powder deposited on the sample fixing table was cut out using Ga ion beams, and the flake was transferred to a carbon-coated Cu grid. Cross-sectional high-angle annular dark field scanning transmission electron microscopy (HAADF-STEM) image was obtained on a JEOL JEM-2100F microscope at an accelerating voltage of 200 kV. TG-DTA was conducted using a RIGAKU Thermo Plus EVO2 TG8121 under dry air at a heating rate of 10 K min^{-1}.

3 Results and discussion

3.1 Synthesis of cage siloxanes modified with seven $SiMe_2OH$ and one $SiMe_2C_{18}H_{37}$ groups (D4R-7SiOH-C18)

The first step for the synthesis of **D4R-7SiOH-C18** was dimethylsilylation of $Si_8O_{20}^{8-}$ to form cage siloxane modified with $SiMe_2H$ groups at 7 corners (**D4R-7SiH**). The progress of dimethylsilylation was confirmed by the ^{1}H NMR spectrum of the silylated product (Fig. S1) showing the signals of the $OSiMe_2H$ groups (0.25 and 4.73 ppm) [16]. The ^{29}Si NMR spectrum (Fig. 1A(a)) showed multiple signals at the M^1 ($SiOSiMe_2H$: −0.9 to −1.5 ppm), Q^3 ($Si(OSi)_3OH$: −100.4 to −100.6 ppm), and Q^4 ($Si(OSi)_4$: −108.4 to −108.9 ppm) regions. The integral ratio of the M^1, Q^3, and Q^4 signals was 7.5: 0.5: 7.5, indicating that the average number of dimethylsilylated corners was 7.5 per Si_8O_{20} and the products were mixtures of cage siloxanes with different numbers of silylated corners. Note that mono-/hepta-substituted cage siloxanes consist of four chemically inequivalent Si atoms [29, 30]. In the case of **D4R-7SiH**, the Q^3 signal of the unsilylated SiOH group and the Q^4 signals of the silylated corner Si atoms first, second, and third closest to the SiOH group should be observed with the 1: 3: 3: 1 ratio. The largest Q^4 and M^1 signals were probably derived from the symmetrical cage siloxane modified with eight $SiMe_2H$ groups, and the smaller signals were assumed to be derived from the cage siloxanes modified with six and seven $SiMe_2H$ groups. The MALDI-TOF mass spectrum (Fig. 1B(a))

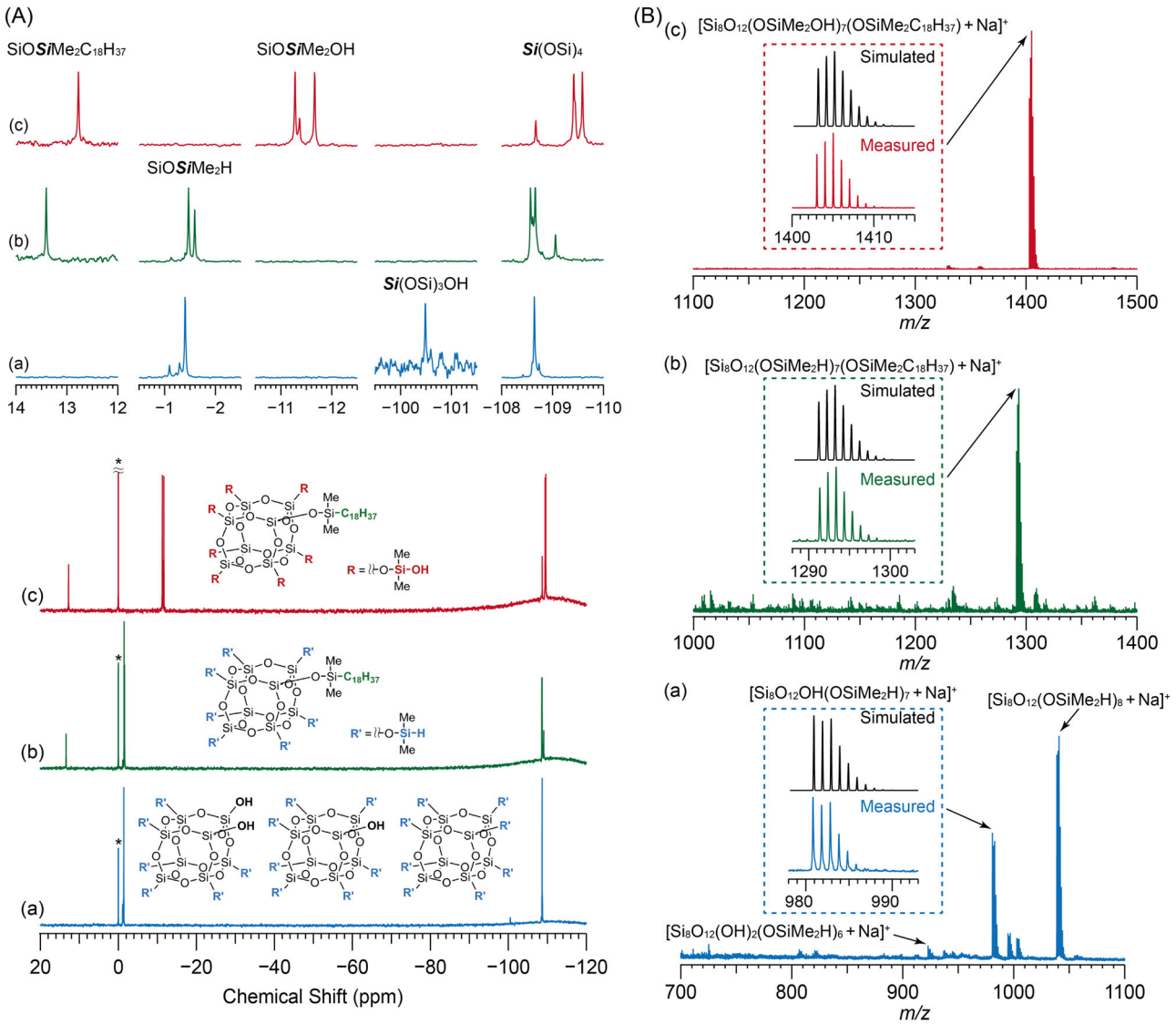

Fig. 1 **A** Liquid-state ^{29}Si NMR spectra and (**B**) MALDI-TOF mass spectra (the insets show the enlarged spectra) of (**a**) dimethylsilylated product containing **D4R-7SiH** (in chloroform-*d*), (**b**) **D4R-7SiH-C18** (in chloroform-*d*), and (**c**) **D4R-7SiOH-C18** (in THF-d_8). The ^{29}Si NMR signals of tetramethylsilane ($\delta = 0$ ppm) are indicated with asterisks (*). The molecular structures of the products are shown in the insets of (Fig. 1**A**). One of the regioisomers is shown for $[Si_8O_{12}(OH)_2(OSiMe_2H)_6]$ (inset of Fig. 1A(a))

showed the peaks corresponding to $[Si_8O_{12}(OH)_2(OSiMe_2H)_6 + Na]^+$, $[Si_8O_{12}OH(OSiMe_2H)_7 + Na]^+$, and $[Si_8O_{12}(OSiMe_2H)_8 + Na]^+$. These results indicated that the silylated product contained **D4R-7SiH** along with other cage siloxanes modified with 6 and 8 $SiMe_2H$ groups.

The second step was the silylation of the residual silanol group of **D4R-7SiH** with C_{18}DMSCl to form a cage siloxane modified with seven $SiMe_2H$ groups and one $SiMe_2C_{18}H_{37}$ group (**D4R-7SiH-C18**). The crude product was separated by GPC (Fig. S2) to obtain **D4R-7SiH-C18**. The ^{1}H NMR spectrum (Fig. S3) showed the signals for $OSi(CH_3)_2C_{18}H_{37}$ (*a*: 0.13 ppm), $OSi(CH_3)_2H$ (*b*: 0.22–0.29 ppm), $SiC_{18}H_{37}$ (*c*: 0.56–0.62 ppm; *d*: 0.88 ppm; *e*: 1.20–1.40 ppm), and $Si(CH_3)_2H$ (*f*: 4.70–4.76 ppm). The integral ratio of $(a + b)$: $(c + d + e)$: *f* was 48: 37: 7, which was consistent with the theoretical ratio for **D4R-7SiH-C18** (48: 37: 7). The ^{29}Si NMR spectrum (Fig. 1A(b)) showed the signals assigned to the M^1 units of the silyl groups ($OSiMe_2C_{18}H_{37}$: 13.41 ppm; $OSiMe_2H$: −1.47 and −1.59 ppm) and the Q^4 units of the cage framework ($Si(OSi)_4$: −108.57, −108.61, −108.66, −109.06 ppm). The disappearance of the Q^3 signals indicated that silylation was complete. The multiple signals observed for $OSiMe_2H$ and $Si(OSi)_4$ can be ascribed to the slight differences in the chemical environments depending on the distance from the $SiMe_2C_{18}H_{37}$ group. One of the M^1 ($SiOSiMe_2H$) signals is likely overlapping with another, resulting in the appearance of only two main signals. The integral ratio of the

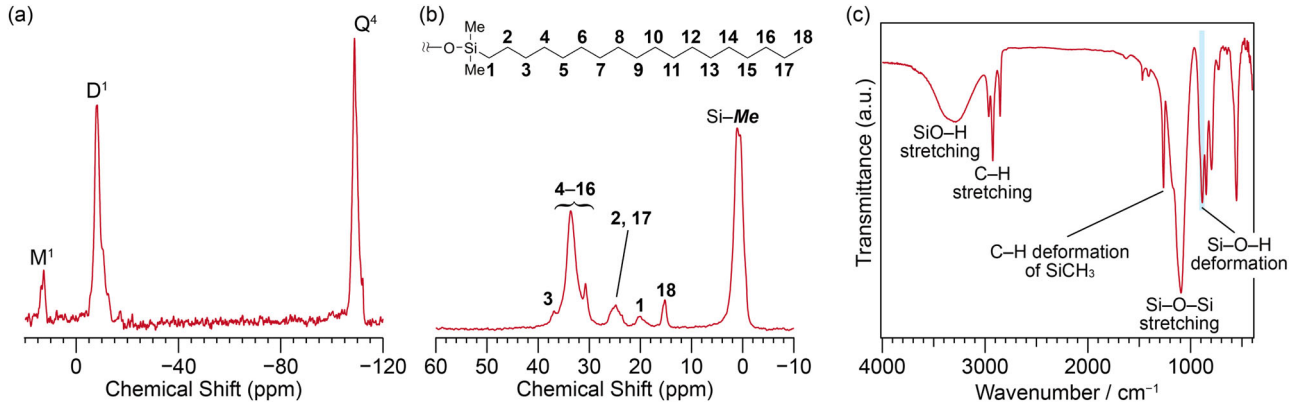

Fig. 2 **a** ^{29}Si MAS NMR spectrum, (**b**) ^{13}C CP/MAS NMR spectrum, and (**c**) FT-IR spectrum of **D4R-7SiOH-C18** assembled by solvent evaporation

O*Si*$Me_2C_{18}H_{37}$, O*Si*Me_2H, and *Si*$(OSi)_4$ signals was 1.0: 7.0: 8.0, indicating that the seven corners were modified with $SiMe_2H$ groups and one corner was modified with a $SiMe_2C_{18}H_{37}$ group. The MALDI-TOF mass spectrum (Fig. 1B(b)) showed the peaks corresponding to $[Si_8O_{12}(OSiMe_2H)_7(OSiMe_2C_{18}H_{37}) + Na]^+$. These results indicated that **D4R-7SiH-C18** was successfully obtained.

The final step was oxidation of the SiH groups of **D4R-7SiH-C18** to form **D4R-7SiOH-C18**. The ^{1}H NMR spectrum of **D4R-7SiOH-C18** (Fig. S4) showed signals for OSi(CH_3)$_2$OH (*a*: 0.10 ppm), OSi(CH_3)$_2C_{18}H_{37}$ (*b*: 0.14 ppm), $SiC_{18}H_{37}$ (*c*: 0.60–0.65 ppm; *d*: 0.88 ppm; *e*: 1.22–1.38 ppm), and Si(CH_3)$_2$O*H* (*f*: 0.55–0.56 ppm; *g*: 0.56–0.57 ppm). The integral ratio of $(a + b)$: $(c + d + e)$: $(f + g)$ was 48: 37: 7, which was consistent with the theoretical ratio for **D4R-7SiOH-C18**. The ^{29}Si NMR spectrum (Fig. 1A(c)) showed a single M^1 signal (O*Si*$Me_2C_{18}H_{37}$: 12.77 ppm), three D^1 signals (O*Si*Me_2OH: −11.28, −11.37, −11.66 ppm), and four Q^4 signals (*Si*$(OSi)_4$: −108.67, −109.42, −109.45 (shoulder), −109.59 ppm). The numbers and the intensity ratios of the D^1 and Q^4 signals are consistent with those in **D4R-7SiOH-C18**. Although detailed signal assignments are difficult, the four Q^4 signals can be attributed to the cage corner Si atoms first, second, third, and fourth closest to the $SiMe_2C_{18}H_{37}$ group (1: 3: 3: 1 ratio). Similarly, the three D^1 signals can be attributed to the Si(CH_3)$_2$OH groups first, second, and third closest to the $SiMe_2C_{18}H_{37}$ group (3: 3: 1 ratio). The MALDI-TOF mass spectrum (Fig. 1B(c)) shows the peak corresponding to $[Si_8O_{12}(OSiMe_2OH)_7(OSiMe_2C_{18}H_{37}) + Na]^+$. The isotope pattern was consistent with that obtained by simulation. These results indicated that the cage siloxane was successfully modified with seven $SiMe_2OH$ groups and one $SiMe_2C_{18}H_{37}$ group.

3.2 Self-assembly of D4R-7SiOH-C18

Self-assembly of **D4R-7SiOH-C18** easily occurred upon solvent evaporation. The ^{29}Si MAS NMR spectrum of the product (Fig. 2(a)) showed the M^1, D^1, and Q^4 signals corresponding to **D4R-7SiOH-C18**. No signal was observed at the D^2 region (around −20 ppm), indicating that the silanol groups remained intact without condensation to form siloxane bonds. This solid product was therefore resoluble in THF. The ^{13}C CP/MAS NMR spectrum (Fig. 2(b)) shows the signals for Si*C*H_3 (0.5 and 1.0 ppm) and $SiC_{18}H_{37}$ (15.2, 20.1, 24.8, 30.7, 33.7, and 36.9 ppm) [31, 32]. The interior methylene carbons of the $C_{18}H_{37}$ groups are observed at 30.4 ppm and 33.8 ppm, which correspond to mixed *trans–gauche* and all-*trans* conformations, respectively [33–35]. Because the latter signal (33.8 ppm) is mainly observed, it is likely that the alkyl chains are in an ordered all-*trans* state with some *gauche* defects. The FT-IR spectrum (Fig. 2(c)) showed bands due to alkyl chains, SiMe groups, SiOH groups, and SiOSi networks. The stretching vibration of the SiO–H groups was observed as a broad band centered at 3295 cm^{-1}, which was attributed to the H-bonded silanol groups [16–19, 36].

The powder XRD pattern of self-assembled **D4R-7SiOH-C18** (Fig. 3a) exhibited the most intense peak at $d = 3.1$ nm along with second- and third-order peaks. These peaks were assignable to a lamellar structure and differed from other mesophases such as 2D hexagonal and cubic phases [37]. In fact, when calcined in air at 250 °C for 1 d to remove alkyl chains, most of the diffraction peaks disappeared (Fig. S5), as in the previously reported lamellar alkylsiloxanes [9]. The *d* value of the first-order peak (3.1 nm) was slightly smaller than the molecular length of **D4R-7SiOH-C18** when the alkyl group is assumed to be all-*trans* (~3.6 nm). Taking into account the relatively large occupying volume of the cage siloxane units, it is reasonable to consider that an interdigitated monolayer-type structure rather than a bilayer-type structure was formed. The other peaks observed at $d = 1.1$ nm and higher angles can be attributed to the arrangements of H-bonded cage siloxanes and

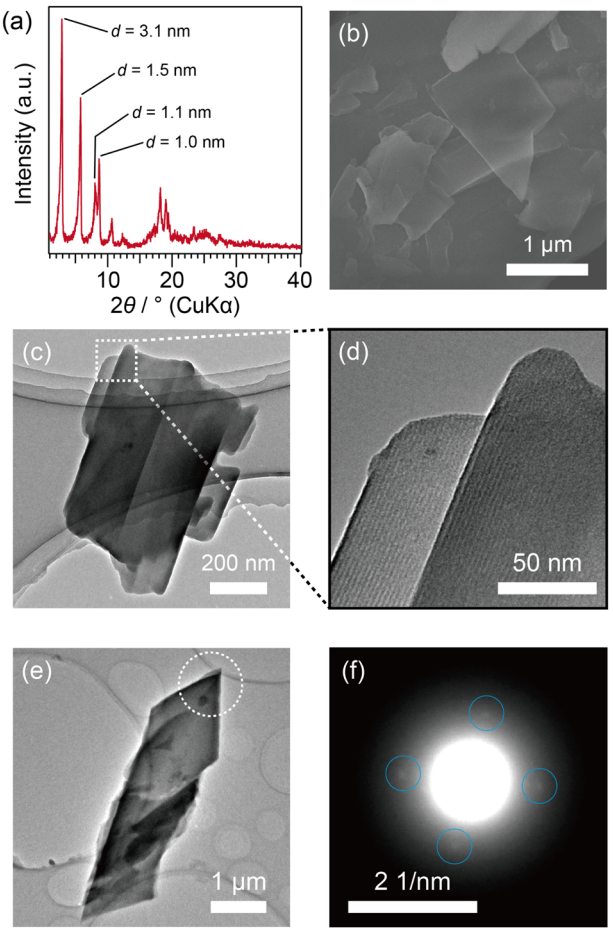

Fig. 3 **a** XRD pattern, (**b**) SEM image, (**c**–**e**) TEM images, and (**f**) SAED pattern (the spots are marked with light blue circles) of self-assembled **D4R-7SiOH-C18**

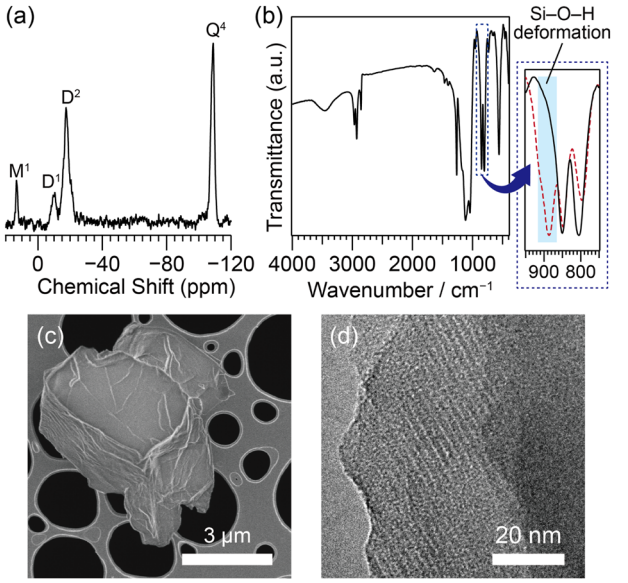

Fig. 4 **a** ^{29}Si MAS NMR spectrum, (**b**) FT-IR spectrum (For comparison, the FT-IR spectrum of **D4R-7SiOH-C18** before the treatment with dichlorodimethylsilane is shown as a dashed line in the enlarged figure.), (**c**) SEM image, and (**d**) TEM image of **D4R-7SiOH-C18** treated by dichlorodimethylsilane

closely packed long alkyl chains. Unfortunately, further information about the molecular arrangement has not been obtained because of the ill-defined peaks and difficulty in the preparation of large crystals for single-crystal X-ray analysis.

The SEM observation revealed that most of the particles have plate-like morphology (Fig. 3b). A stripe pattern characteristic of a lamellar structure was observed near the edge of the particles (Fig. 3c, d). The HAADF-STEM observation of the cross-section of the particle cut vertically by FIB processing also showed a stripe pattern oriented parallel to the particle surface (Fig. S6). The SAED pattern of another view (Fig. 3e, f) showed spots with a *d* value of about 0.95 nm. These spots are likely associated with the H-bonding arrangement of the cage molecules because similar square arrays of spots were reported for the H-bonded molecular crystals of D4R siloxanes modified with $SiMe_2OH$ groups at all corners [16, 17]. All the above results suggested that the cage siloxanes were arranged to form a molecularly and mesoscopically ordered structure.

3.3 Cross-linking of D4R-7SiOH-C18 by silylation

The self-assembled solids of **D4R-7SiOH-C18** were treated with dichlorodimethylsilane to bridge the adjacent silanol groups by siloxane bonds. The solid-state ^{29}Si MAS NMR spectrum of the product (Fig. 4a) showed the M^1 ($OSiMe_2C_{18}H_{37}$: 13.2 ppm), D^1 ($OSiMe_2OH$: −10.3 ppm), D^2 ($SiMe_2(OSi)_2$: −17.5 ppm), and Q^4 ($Si(OSi)_4$: −108.9 ppm) signals. The sharp Q^4 signal accompanying no Q^3 signal suggested that the silylated cage siloxane units were almost retained without cleavage of the Si–O–Si bonds. The integral ratio of M^1, D^1, D^2, and Q^4 signals was calculated to be 1.0: 1.7: 7.7: 8.0. Assuming that one dichlrodimethylsilane reacts with two silanol groups, the theoretical ratio of M^1, D^2, and Q^4 units is calculated to be 1.0: 10.5: 8.0. The difference between the theoretical and measured ratios indicated that ~75% of the silanol groups underwent cross-linking. FT-IR analysis also confirmed that the band assignable to Si–O–H deformation (887 cm^{-1}) significantly decreased (Fig. 4b). After silylation, the XRD peaks observed for **D4R-7SiOH-C18** became weak and/or broad, and no new peaks appeared (Fig. S7). Sheet-like morphology was still observed by SEM (Fig. 4c) and stripe patterns were observed by TEM (Fig. 4d). These results suggested that the lamellar structure was at least partially retained after the cross-linking. We expect that the structural regularity can be improved by optimizing the reaction conditions and/or by the choice of the silylating agent used.

The synthetic method of crystalline 2D silica-based materials presented in this study will be useful for the

preparation of functional coatings and membranes. The structure of the siloxane frameworks is the critical factor for these applications. Until now, the top-down synthesis of crystalline silica nanosheets by exfoliation of 2D zeolites [38] and layered silicates [39], as well as their applications for barrier coatings and gas separation membranes, have been reported. However, the types of structures that can be obtained by exfoliation of those hydrothermally synthesized layered compounds are limited. The surfactant-directed self-assembly process allows for the preparation of lamellar silica- and organosiloxane-based materials [40–42], and a recent report has shown that colloidal silica nanosheets can be obtained by exfoliation [43]. However, these materials have amorphous siloxane networks unless post-synthetic hydrothermal treatment is employed [44]. The bottom-up self-assembly method using well-defined cage siloxanes has the potential to overcome these limitations, although further research is needed to retain the crystal structure upon cross-linking. The direct formation of single-layer nanosheets may also be possible by the Langmuir–Blodgett technique.

4 Conclusions

We have demonstrated the hierarchical assembly of cage siloxane building blocks by hydrophobic interactions and hydrogen bondings. A long-chain alkyl group and organosilanol groups were successfully introduced to cage siloxane with a D4R structure by stepwise silylation using chlorodimethylsilane and chloro(octadecyl)dimethylsilane followed by conversion of the SiH groups into SiOH groups. Self-assembly of the resulting compound, **D4R-7SiOH-C18**, occurred upon solvent evaporation. Furthermore, cross-linking of **D4R-7SiOH-C18** using dichlorodimethylsilane proceeded while retaining the sheet-like morphology. This approach will allow for the creation of various hierarchically ordered siloxane-based materials by the molecular design of the building blocks.

Acknowledgements We thank Dr. Toshimichi Shibue (MCCL, Waseda University) for solid-state NMR analysis [45], Dr. Noriko Hanzawa, Mr. Toshiyuki Akanuma (Kagami Memorial Research Institute for Materials Science and Technology, Waseda University), Mr. Tetsuya Hattori, Mr. Takumi Houya (Waseda University) for electron microscopic analyses, Mr. Masashi Yatomi, and Mr. Yoshiaki Miyamoto (Waseda University) for fruitful discussion. This work was supported in part by JSPS KAKENHI Grant Number 23H02051. The NMR and mass analyses using JEOL JNM ECZ 500, JEOL JNM ECA 400, and Bruker autoflex maX: Material Characterization Central Laboratory were supported by MEXT Project for promoting public utilization of advanced research infrastructure (Program for supporting construction of core facilities) (Grant Number JPMXS0440500022). XRD and electron microscopic analyses are the results of using research equipment (Rigaku Ultima-III, Hitachi S5500, JEOL JEM-2010, JEOL JEM-2100F, and JEOL JIB-4700F) of Kagami Memorial Research Institute for Materials Science and Technology.

Supplementary information The online version contains supplementary material available at https://doi.org/10.1007/s10971-023-06184-w.

References

1. Davis ME (2002) Ordered porous materials for emerging applications. Nature 417(6891):813–821. https://doi.org/10.1038/nature00785
2. Cundy CS, Cox PA (2003) The hydrothermal synthesis of zeolites: History and development from the earliest days to the present time. Chem Rev 103(3):663–702. https://doi.org/10.1021/cr020060i
3. Takahashi N, Kuroda K (2011) Materials design of layered silicates through covalent modification of interlayer surfaces. J Mater Chem 21(38):14336–14353. https://doi.org/10.1039/C1JM10460H
4. Liu Y, Chaiprasert T, Ouali A, Unno M (2022) Well-defined cyclic silanol derivatives. Dalton Trans 51(11):4227–4245. https://doi.org/10.1039/D1DT04270J
5. Unno M, Matsumoto T (2013) Laddersiloxanes–silsesquioxanes with defined ladder structure. Russ Chem Rev 82(4):289–302. https://doi.org/10.1070/RC2013v082n04ABEH004360
6. Kinoshita S, Watase S, Matsukawa K, Kaneko Y (2015) Selective synthesis of cis–trans–cis cyclic tetrasiloxanes and the formation of their two-dimensional layered aggregates. J Am Chem Soc 137(15):5061–5065. https://doi.org/10.1021/jacs.5b00319
7. Laine RM (2005) Nanobuilding blocks based on the $[OSiO_{1.5}]_x$ (x = 6, 8, 10) octasilsesquioxanes. J Mater Chem 15(35-36):3725–3744. https://doi.org/10.1039/B506815K
8. Cordes DB, Lickiss PD, Rataboul F (2010) Recent developments in the chemistry of cubic polyhedral oligosilsesquioxanes. Chem Rev 110(4):2081–2173. https://doi.org/10.1021/cr900201r
9. Shimojima A, Kuroda K (2006) Designed synthesis of nanostructured siloxane–organic hybrids from amphiphilic silicon-based precursors. Chem Rec 6(2):53–63. https://doi.org/10.1002/tcr.20073
10. Suzuki J, Shimojima A, Fujimoto Y, Kuroda K (2008) Stable silanetriols that contain tert-alkoxy groups: versatile precursors of siloxane-based nanomaterials. Chem Eur J 14(3):973–980. https://doi.org/10.1002/chem.200700914
11. Soldatov M, Liu H (2021) Hybrid porous polymers based on cage-like organosiloxanes: synthesis, properties and applications. Prog Polym Sci 119:101419. https://doi.org/10.1016/j.progpolymsci.2021.101419
12. Hu N-H, Sims CB, Schrand TV, Haver KM, Armenta HE, Furgal JC (2022) Formation of nanostructured silicas through the fluoride catalysed self-polymerization of Q-type functional silica cages. Chem Commun 58(72):10008–10011. https://doi.org/10.1039/D2CC02672D
13. Kawakami Y, Sakuma Y, Wakuda T, Nakai T, Shirasaka M, Kabe Y (2010) Hydrogen-bonding 3D networks by polyhedral organosilanols: selective inclusion of hydrocarbons in open frameworks. Organometallics 29(15):3281–3288. https://doi.org/10.1021/om901120m

14. Nozawa T, Matsumoto T, Yagihashi F, Beppu T, Sato K, Igarashi M (2018) $[Si_8O_{12}][OH]_8$: Isolation, structure, and reactivity of a cubic octamer of orthosilicic acid. Chem Lett 47(12):1530–1533. https://doi.org/10.1246/cl.180776
15. Igarashi M, Nozawa T, Matsumoto T, Yagihashi F, Kikuchi T, Sato K (2021) Parallel-stacked aromatic molecules in hydrogen-bonded inorganic frameworks. Nat Commun 12(1):7025. https://doi.org/10.1038/s41467-021-27324-2
16. Sato N, Kuroda Y, Abe T, Wada H, Shimojima A, Kuroda K (2015) Regular assembly of cage siloxanes by hydrogen bonding of dimethylsilanol groups. Chem Commun 51(55):11034–11037. https://doi.org/10.1039/C5CC03668B
17. Sato N, Kuroda Y, Wada H, Shimojima A, Kuroda K (2018) Preparation of siloxane-based microporous crystals from hydrogen-bonded molecular crystals of cage siloxanes. Chem Eur J 24(64):17033–17038. https://doi.org/10.1002/chem.201804441
18. Sato N, Tochigi K, Kuroda Y, Wada H, Shimojima A, Kuroda K (2019) Synthesis and crystal structure of double-three ring (D3R)-type cage siloxanes modified with dimethylsilanol groups. Dalton Trans 48(6):1969–1975. https://doi.org/10.1039/C8DT04244F
19. Sato N, Kuroda Y, Wada H, Shimojima A, Kuroda K (2021) Hydrogen-bonding-induced layered assembly of cage siloxanes modified with diisopropylsilanol groups. Chem Lett 50(10):1770–1772. https://doi.org/10.1246/cl.210387
20. Knischka R, Dietsche F, Hanselmann R, Frey H, Mülhaupt R, Lutz PJ (1999) Silsesquioxane-based amphiphiles. Langmuir 15(14):4752–4756. https://doi.org/10.1021/la981594a
21. Chen F, Lin F, Zhang Q, Cai R, Wu Y, Ma X (2019) Polyhedral oligomeric silsesquioxane hybrid polymers: Well-defined architectural design and potential functional applications. Macromol Rapid Commun 40(17):1900101. https://doi.org/10.1002/marc.201900101
22. Yin G-Z, Zhang W-B, Cheng SZD (2017) Giant molecules: where chemistry, physics, and bio-science meet. Sci China Chem 60(3):338–352. https://doi.org/10.1007/s11426-016-0436-x
23. Shimojima A, Goto R, Atsumi N, Kuroda K (2008) Self-assembly of alkyl-substituted cubic siloxane cages into ordered hybrid materials. Chem Eur J 14(28):8500–8506. https://doi.org/10.1002/chem.200801106
24. Goto R, Shimojima A, Kuge H, Kuroda K (2008) A hybrid mesoporous material with uniform distribution of carboxy groups assembled from a cubic siloxane-based precursor. Chem Commun (46):6152–6154. https://doi.org/10.1039/B813679C.
25. Hagiwara Y, Shimojima A, Kuroda K (2008) Alkoxysilylated-derivatives of double-four-ring silicate as novel building blocks of silica-based materials. Chem Mater 20(3):1147–1153. https://doi.org/10.1021/cm0716194
26. Hasegawa I, Motojima S (1992) Dimethylvinylsilylation of $Si_8O_{20}^{8-}$ silicate anion in methanol solutions of tetramethylammonium silicate. J Organomet Chem 441(3):373–380. https://doi.org/10.1016/0022-328X(92)80168-W
27. Hasegawa I, Ishida M, Motojima S (1994) Synthesis of silylated derivatives of the cubic octameric silicate species $Si_8O_{20}^{8-}$. Synth React Inorg Met - Org Chem 24(7):1099–1110. https://doi.org/10.1080/00945719408001386
28. Kawakami Y, Seino H, Ohtaki K, Kabe Y (2017) Synthetic application of silicates/silanolates and their hydrolyzed polysilanol siloxanes for polyhedral oligomeric silsesquioxanes (POSSs). Heteroatom Chem 28(3):e21373. https://doi.org/10.1002/hc.21373
29. Saito S, Yamasue N, Wada H, Shimojima A, Kuroda K (2016) Cubic siloxanes with Both Si−H and Si−OtBu groups for site-selective siloxane bond formation. Chem Eur J 22(39):13857–13864. https://doi.org/10.1002/chem.201601906
30. Kajiya R, Sakakibara S, Ikawa H, Higashiguchi K, Matsuda K, Wada H, Kuroda K, Shimojima A (2019) Inorganic–organic hybrid photomechanical crystals consisting of diarylethenes and cage siloxanes. Chem Mater 31(22):9372–9378. https://doi.org/10.1021/acs.chemmater.9b02941
31. Shah P, Rogers LB, Fetzer JC (1987) Differences in carbon 13 nuclear magnetic resonance spectra for monomeric and polymeric octadecyl derivatized silica column packings for liquid chromatography. J Chromatogr A 388:411–419. https://doi.org/10.1016/S0021-9673(01)94501-7
32. Fatunmbi HO, Bruch MD, Wirth MJ (1993) Silicon-29 and carbon-13 NMR characterization of mixed horizontally polymerized monolayers on silica gel. Anal Chem 65(15):2048–2054. https://doi.org/10.1021/ac00063a020
33. Gao W, Reven L (1995) Solid-state NMR studies of self-assembled monolayers. Langmuir 11(6):1860–1863. https://doi.org/10.1021/la00006a007
34. Gao W, Dickinson L, Grozinger C, Morin FG, Reven L (1997) Order−disorder transitions in self-assembled monolayers: A ^{13}C solid-state NMR study. Langmuir 13(2):115–118. https://doi.org/10.1021/la960808q
35. Bisio C, Carniato F, Paul G, Gatti G, Boccaleri E, Marchese L (2011) One-pot synthesis and physicochemical properties of an organo-modified saponite clay. Langmuir 27(11):7250–7257. https://doi.org/10.1021/la200892d
36. Sato Y, Hayami R, Gunji T (2022) Characterization of NMR, IR, and Raman spectra for siloxanes and silsesquioxanes: a mini review. J Sol-Gel Sci Technol 104(1):36–52. https://doi.org/10.1007/s10971-022-05920-y
37. Barton TJ, Bull LM, Klemperer WG, Loy DA, McEnaney B, Misono M, Monson PA, Pez G, Scherer GW, Vartuli JC, Yaghi OM (1999) Tailored porous materials. Chem Mater 11(10):2633–2656. https://doi.org/10.1021/cm9805929
38. Varoon K, Zhang X, Elyassi B, Brewer DD, Gettel M, Kumar S, Lee JA, Maheshwari S, Mittal A, Sung C-Y, Cococcioni M, Francis LF, McCormick AV, Mkhoyan KA, Tsapatsis M (2011) Dispersible exfoliated zeolite nanosheets and their application as a selective membrane. Science 334(6052):72–75. https://doi.org/10.1126/science.1208891
39. Dakhchoune M, Villalobos LF, Semino R, Liu L, Rezaei M, Schouwink P, Avalos CE, Baade P, Wood V, Han Y, Ceriotti M, Agrawal KV (2021) Gas-sieving zeolitic membranes fabricated by condensation of precursor nanosheets. Nat Mater 20(3):362–369. https://doi.org/10.1038/s41563-020-00822-2
40. Huo Q, Margolese DI, Stucky GD (1996) Surfactant control of phases in the synthesis of mesoporous silica-based materials. Chem Mater 8(5):1147–1160. https://doi.org/10.1021/cm960137h
41. Ogawa M (1997) Preparation of layered silica−dialkyldimethylammonium bromide nanocomposites. Langmuir 13(6):1853–1855. https://doi.org/10.1021/la9608775
42. Kodama S, Miyamoto Y, Itoh S, Miyata T, Wada H, Kuroda K, Shimojima A (2021) Self-healing lamellar silsesquioxane thin films. ACS Appl Polym Mater 3(8):4118–4126. https://doi.org/10.1021/acsapm.1c00592
43. Yamamoto E, Fujihara K, Takezaki Y, Ito K, Shi Y, Kobayashi M, Osada M (2023) Free-standing molecularly thin amorphous silica nanosheets. Small 19(22):2300022. https://doi.org/10.1002/smll.202300022
44. Christiansen SC, Zhao D, Janicke MT, Landry CC, Stucky GD, Chmelka BF (2001) Molecularly ordered inorganic frameworks in layered silicate surfactant mesophases. J Am Chem Soc 123(19):4519–4529. https://doi.org/10.1021/ja004310t
45. Izutani C, Fukagawa D, Miyasita M, Ito M, Sugimura N, Aoyama R, Gotoh T, Shibue T, Igarashi Y, Oshio H (2016) The materials characterization central laboratory: An open-ended laboratory program for fourth-year undergraduate and graduate students. J Chem Educ 93(9):1667–1670. https://doi.org/10.1021/acs.jchemed.6b00161